Stopping a Roller Coaster Train.

Ann-Marie Pendrill[1,2] and Magnus Karlsteen[3] and Henrik Rödjegård[4]

1) Department of Physics, University of Gothenburg, SE 412 96 Göteborg, Sweden
2) National Resource Centre for Physics Education, Lund University, Box 118, SE 221 00 LUND, Sweden
3) Department of Applied Physics, Chalmers University of Technology, SE 412 96 Göteborg, Sweden
4) Rödjegård Technology, Norrgårdsvägen 2, SE 820 64, Näsviken, Sweden

E-mail: `Ann-Marie.Pendrill@fysik.lu.se`

Abstract. A roller coaster ride comes to an end. Magnets on the train induce eddy currents in the braking fins, giving a smooth rise in braking force as the remaining kinetic energy is absorbed by the brakes and converted to thermal energy. In this paper an IR camera was used to monitor the temperature of the first braking fin, before, during and after the passage of a train. In addition, the resulting acceleration of the train was modelled and compared to accelerometer data for the Kanonen roller coaster in Liseberg. The results are used to model the distribution of temperature increase over the braking fins. Finally, the cooling of the fins after the passage of the train is analysed and compared to the IR data.

Accepted for publication in *Physics Education* Nov 2012. Online supplementary data available from stacks.iop.org/PhysED/47/000/mmedia

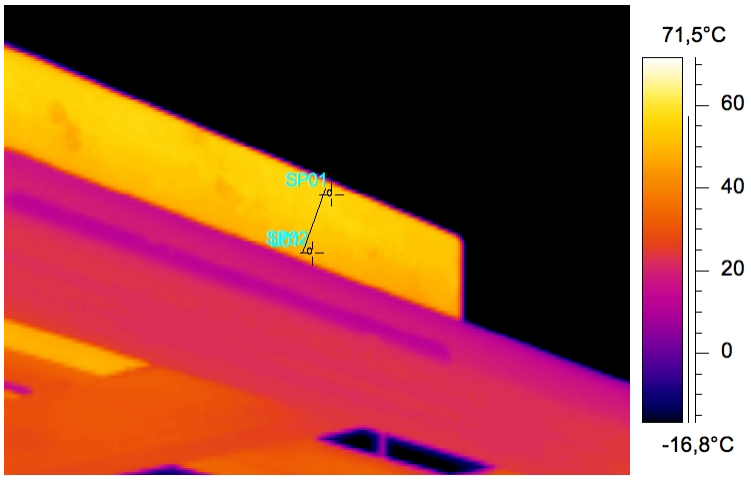

Figure 1. IR image of the first braking fin after a train has passed. The two points marked are used for extracting the time-dependence of the temperature.

1. Introduction

Roller coasters are classical examples of energy conversion, with an interplay of kinetic and potential energy as the train moves around the curves, loops, hills and valleys of the track. At the end of the ride, the train must be slowed down and brought to a stop in the station. In modern roller coasters, permanent magnets on the train (or track) induce eddy currents in braking fins as the train moves past the brakes [1]. The faster the train, the stronger the currents induced, and the stronger the braking force. The onset of the braking is smooth; as the train enters the brakes, more and more braking fins are activated. This is in strong contrast to the sudden action of older roller coaster brakes.

The kinetic energy of the roller coaster train is converted to thermal energy in the braking system. A large fraction of the energy is absorbed by the braking fins - sheets of brass along the brake run - leading to a temperature increase. We have used an IR camera to study this temperature increase in the first brake fin of the Kanonen roller coaster at the Liseberg amusement park in Göteborg, Sweden [2, 3], as discussed in section 2. The subsequent cooling is discussed in section 5.

Since the speed of the train is reduced by the brakes, stronger eddy currents are produced in the earlier brake fins and more energy is absorbed than in the later brake fins. To find how the temperature increase varies over the length of the brakes, we have modelled the stopping of a train entering the brake run (section 3 and Appendix A). The results from the model were then compared to authentic accelerometer data in the Kanonen roller coaster (section 4). The comparison also gave suitable numeric data for the pre-braking speed and the braking force. The resulting time dependence of the acceleration (i.e. the slowing down) of the train, as well as speed and distance from the model were then used to model the energy distribution over the brake run (section 4.1 and Appendix B).

2. Heating of the braking fins

The kinetic energy of the train before the brakes, $E_k = mv_0^2/2$, is converted into thermal energy. What temperature increase would result if we assume that all the energy is absorbed by the brass plates in the braking fins? To estimate this increase we need to know the masses involved. The mass of the train in Kanonen train is around 7000 kg. The initial speed of the train is estimated to $v_0 \approx 12$ m/s, based on the matching to the accelerometer data discussed in section 4, and consistent with data from the technical drawing, and from on-site timing of the passage of the train. The brakes consisted of 9 pairs of braking fins, each with a length $L = 0.825$m, and $h = 0.200$m high and $b = 6$mm thick. The last pair was only 0.600m long. (Additional brake fins have been added after the measurements.) The brass used in the fins is CuZn10, except for the last ones, were CuZn5 was used, i.e. consisting mainly of copper, but containing, respectively 10% and 5% zinc. The presence of zinc leads to a small reduction of the density, to

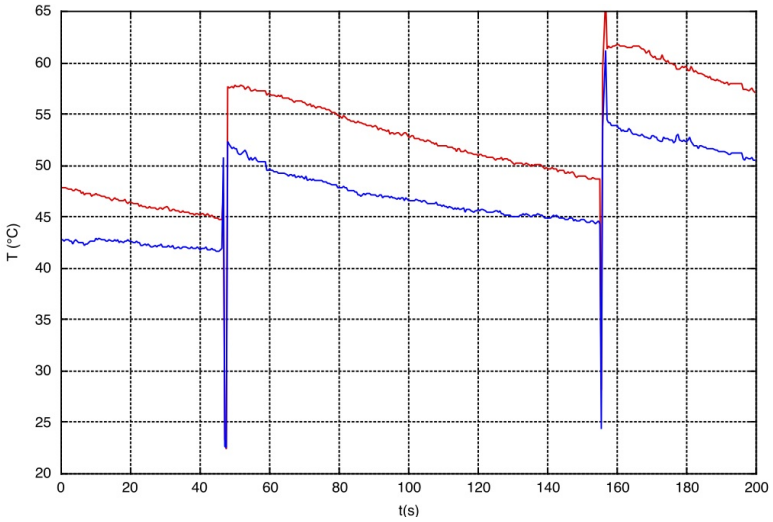

Figure 2. Time dependence of the temperature (in ^{o}C) of the brakes in Kanonen before and after two train passages. The dips in temperature are caused by the colder train obscuring the brakes during the passage itself. The blue (upper) and red (lower) graphs correspond, respectively, to the upper and lower points marked in figure 1 .

$\rho = 8.74 \times 10^3 \mathrm{kg}/m^3$ compared to the value $8.96 \times 10^3 \mathrm{kg}/m^3$ for copper. The specific heat $C = 385$ J$/kgK$ remains essentially unchanged. The zinc admixture leads to a significant reduction of the electric conductivity [4]; the lower zinc content in the last few brake fins thus leads to an increase in their braking power.

A temperature increase of $E_k/C\rho V = E_k/C\rho(18Lhb) \approx 8.4$K could be expected if all the kinetic energy were absorbed by the brake fins and evenly distributed. However, the train passes the first brake fins with larger speed than the following ones, so we expect more energy deposited there. To analyse the temperature increase distribution, we need to know in more detail how the train slows down, as discussed in the next section.

Figure 2 shows the time dependence of temperature in two points of the first brake fin before and after two train passages, indicating an increase of 9-13 K when a train passes. During the passage, the train obscures the brake, giving a dip in the temperature reading. In addition, there is a very brief reading of higher temperature. We interpret this as a skin effect, where currents and heating have not yet penetrated through the whole thickness of the sheet. We can also see from the IR movie [5] that the initial heating is concentrated at the center of the surface.

3. Modelling the deceleration of the train

In the discussion below, we assume that the magnets are placed on the train and the braking fins placed on the track, as in the Kanonen roller coaster. The opposite arrangement is possible and used in other roller coasters, as discussed in Ref.[1]. However, the mathematics or physics does not depend on the choice of technology.

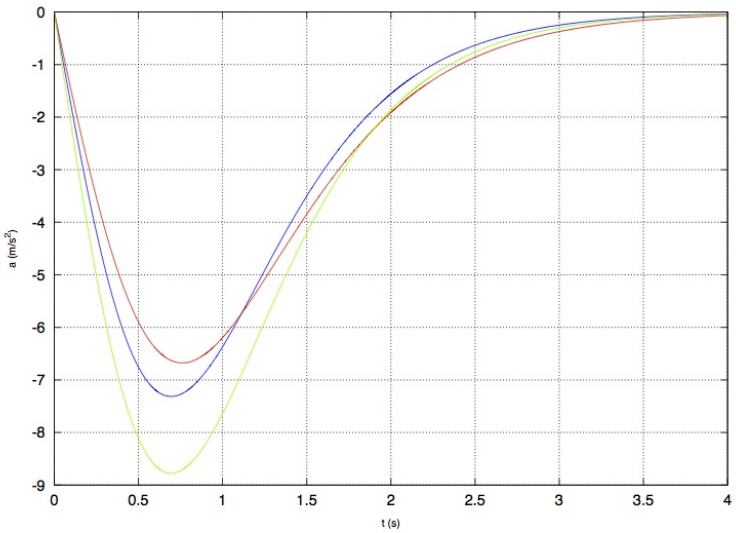

Figure 3. Acceleration vs time for a train entering a horizontal brake run with initial speed $v_0 = 12$ m/s (green) or 10 m/s (red and blue) and with the values $k = 0.15$ /(ms) (red and green) and $k = 0.18$ /(ms) (blue curve).

The magnetic brake run is a straight line so the motion in this part of the ride is purely one-dimensional.

To model the acceleration of the train first note that the induced electric field is proportional to the time derivative of the magnetic field, in turn proportional to the speed, v, of the magnet. The induced eddy current in a conductor is proportional to the resulting electric field, in turn leading to an induced magnetic field proportional to the speed. The current is also proportional to the conductivity, σ, of the material in the braking fin. Collecting these factors we can express the force from a conductor on a moving magnet as $F \propto \sigma B^2 v$ [6]. In the case of a linear magnetic brake, the force is also proportional to the length where magnets are adjacent to the braking fins, which corresponds to the distance, s, the train has traveled into the brake run. Since $\mathbf{a} = \mathbf{F}/m$ we can write

$$a = -kvs \tag{1}$$

The minus sign indicates that the acceleration is opposite to the direction of motion, causing the train to slow down. The properties of the magnets, the material and dimensions of the braking fins, as well as the distance between them, enter in the constant, k. This constant also depends on the mass of the train; a fully loaded train will come to a stop more slowly than an empty train. (For very rapidly changing magnetic fields, the eddy currents do not penetrate the whole conductor. The thickness of 6 mm of the braking swords is the skin thickness corresponding to a frequency of about 100 Hz for the variation of the magnetic field. The magnets on the Kanonen train are mounted in 0.5m yokes, each containing 6 magnets, giving frequencies of this order of magnitude for the change in magnetic field. We do not consider skin effects in

our analysis.)

As a first approximation, we assume that there brakes and train are "infinitely long", or rather, sufficiently long for the train to come to a stop before the front of the train has moved past the end of the brakes, and before the tail of the train has reached the start of the brake run. Figure 3 shows how the acceleration varies with time for this approximation for a few values of the constant k and the initial speed, v_0. The different graphs in Figure 3 can, in fact, be joined into a single graph by introducing dimensionless variables, as discussed in more detail in Appendix A, which also gives an analytical solution for the case of a long train on a horizontal track. Figure 4 shows how acceleration and speed varies with distance, all expressed in the corresponding dimensionless variables.

It is interesting to note that, although the braking power is reduced with decreased speed, which never reaches zero, the train only moves a finite length. Design concerns may include how the acceleration varies with distance travelled and not least how the stopping distance depends on the initial speed, on the number of passengers in the train and possibly on other variables.

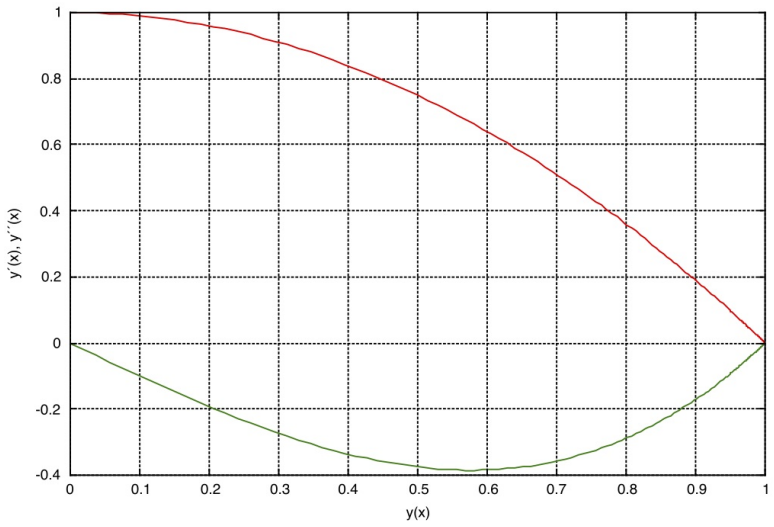

Figure 4. Acceleration and speed vs distance as the train enters the brake run for a horizontal track. The graph uses the dimensionless variables, presented in the appendix, i.e. $y = s\sqrt{2k/v_0}$, $y' = v/v_0$ and $y'' = a/\sqrt{kv_0^3}$.

4. Stopping a real roller-coaster train

How well does the model describe the actual acceleration of a real roller coaster train? For comparison, we choose the Kanonen roller coaster at the Liseberg amusement park in Gothenburg, Sweden [2, 3], which has also been studied in earlier work [7, 8]. The train is 9.8 m long. At the time of the measurement, there were 9 pairs of braking fins with a total length of 7.2m. The magnetic braking power is thus reduced, first when

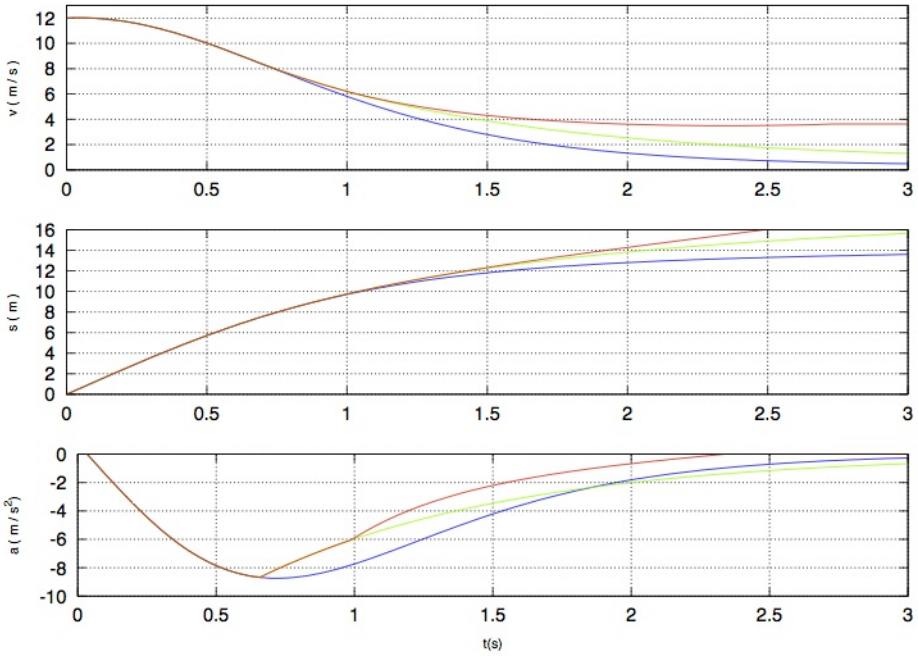

Figure 5. Time dependence of speed, distance and acceleration after the roller coaster train enters the magnetic brake. The blue curves would hold if train and brakes were sufficiently long for the train to come to a stop without reaching the end of train or brakes. The green curve accounts for the finite length of the brakes and the red curve also takes into account the finite length of the train.

the front of the train reaches the end of the brakes, and then even more when the end of the train reaches the start of the brake.

The results in section 3 were obtained for a horizontal track. However, the track in the Kanonen has a forward slope of 4.3^o. This small slope ensures that the train continues to move until it reaches the station. This obviously leads to a slightly slower stopping, which has been accounted for in the numerical simulations presented here. It also causes the acceleration to be slightly positive until the train has entered a small distance into the brakes. The resulting data for speed, distance and acceleration are shown in Figure 5.

Figure 6 shows a comparison of experimental acceleration data with values obtained from the modeling. The accelerometer measures the component along the track of the vector $\mathbf{a} - \mathbf{g}$. The data in the figure has been compensated for the component, $-g \sin\theta$, of the acceleration of gravity. An essential part of the data analysis is the transformation of coordinates to ensure that one of the coordinate axes coincides with the direction of the track. This was possible for the data obtained with the motion tracker that was used also in earlier work where acceleration and rotation data for the Balder roller coaster were analysed [9]. This motion tracker is basically a three axis accelerometer and a three axis gyroscope unit. In addition a three axis inclinometer is integrated for proper levelling at start which allows compensation for components of

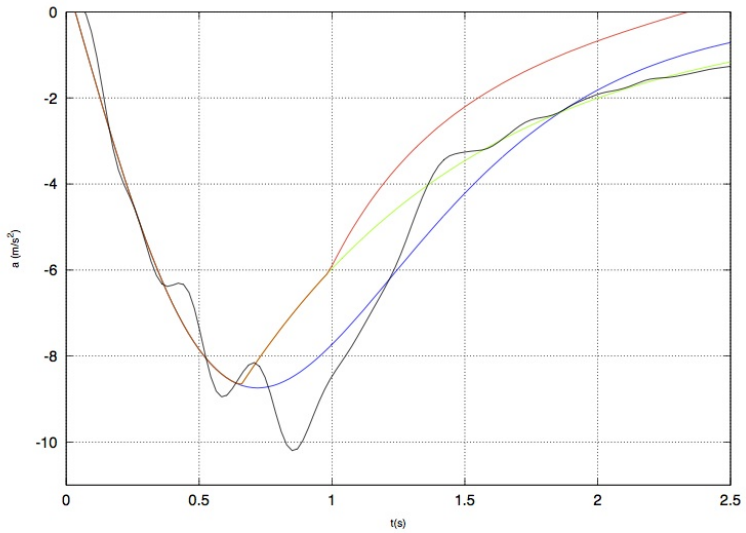

Figure 6. Time dependence of the acceleration after the roller coaster train enters the magnetic brake for $v_0 = 12$m/s and $k = 0.15$/ms for a track with a slope of 4.3^o. The blue curves would apply if train and brakes were sufficiently long for the train to come to a stop without reaching the end of train or brakes. The green curve accounts for the finite length of the brakes and the red curve also takes into account the finite length of the train. The black graph shows the experimental data compensated for the component of g along the track, and the modeling includes the acceleration due to the slope.

g. The gyroscopes, that measure angular velocity, makes it possible to compensate the measured linear acceleration for centripetal acceleration and for the changing direction of the acceleration of gravity relative to the sensor. A simpler accelerometer could have been used if the sensor could have be aligned with the track during the whole brake run.

A short distance after the braking fins, the train enters a system of wheels controlling the final motion of the train into the station. From the data in figure 6 we observe that the effect of the braking wheels to a large extent compensates for the finite length of train and magnetic brakes. This feature of the brake design, makes it possible for us to use the results obtained for long trains and brakes in the analyses below, in spite of the actual finite length.

4.1. Brake fin temperature increase

A temperature increase of $\Delta T = E_k/C\rho(18Lhb) \approx 8.4$K could be expected if all the kinetic energy were absorbed by the brake fins and evenly distributed, as discussed in section 2. However, the first brake fin should heat up more, since the train has higher speed as it passes. The temperature was modelled by evaluating the reduction in kinetic energy lost as the train travels a distance ds and distributing the energy over the part of the brake that is active during this part of the motion. The details of the calculation are shown in Appendix B. Figure 7 shows the expected distribution of temperature

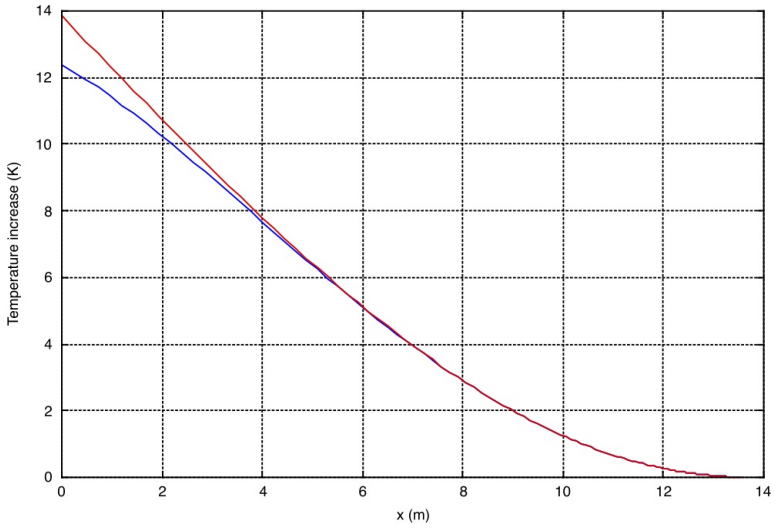

Figure 7. The expected distribution of temperature increase over the brake fins, obtained from the integral in Eq.(B.1). The blue curve takes into account that the brake fins in the beginning of the brake do not contribute to the braking after the train tail has past - this energy would instead be taken up by the mechanical brakes that follow after the brake fins. The data also accounts for the 4.3^o forward slope of the track.

increase over the length of the brake. The largest temperature increase is found to be

$$\Delta T(0) = \frac{m}{3\ C\ \rho h b}\ \sqrt{k 2 v_0^3}.$$

The real temperature increase is slightly lower: Due to the finite length of the train, part of the energy is absorbed by the mechanical brakes following after the braking fins.

5. Cooling down

The brakes must cool down before the next train arrives. The warm fins at temperature T will radiate energy according to Stefan-Boltzmann's law. The net radiation loss to the colder surrounding at temperature T_0 from an area A can be expressed as

$$P = e\sigma A(T^4 - T_0^4) \tag{2}$$

where Stefan's constant $\sigma = 5.6703 \times 10^{-8}\mathrm{W}/m^2K^2$ and e is the emissivity, assumed to be 1. For a distance ds of the braking fins, the area is $A = 2h\ ds$ (accounting for back and front of the fin, but neglecting the small area at the top/bottom edges of the fin). The corresponding volume that is cooling down is $V = hb\ ds$. The rate of temperature change can then be written as

$$\frac{dT}{dt} = \frac{-PA}{C\rho V} = \frac{2e\sigma(T_0^4 - T^4)}{C\rho b} \tag{3}$$

The surrounding temperature can be approximated by the lowest temperature readings in figure 2 for the dips corresponding to the temperature of the passing train. For a fin

temperature 40K higher than a surrounding temperature of 296K, we find a cooling rate due to radiation of about 0.03K/s, which can be seen as an upper limit of the cooling rate due to radiation.

The experimental data from the FLIR camera for the cooling of the first braking fin in figure 2 show the temperature dropping at a rate

$$\frac{dT}{dt} \approx -0.10 K/s. \tag{4}$$

From this comparison, we conclude that other energy losses are more important; to the surrounding air, through convection and wind, and into the track, through conduction, as visible also in the IR movie [5].

6. Discussion

Educational aspects of energy conversions in roller coasters are traditionally limited to the conversion between potential and kinetic energy and possibly discussions of losses along the track. With this work, we demonstrate that energy considerations in roller coaster can involve many more areas of physics and use theory, modeling and measurements in realistic comparisons with real roller coaster data. More detailed studies could also e.g. include video-analysis of the stopping train, as well as measurement of the magnetic field strengths and simulations of the induced eddy currents.

Acknowledgements

We gratefully acknowledge the support by Liseberg, including access to Kanonen when the park was closed, giving us the opportunity to take the relevant IR pictures. Special thanks go to Ulf Johansson and Kenneth Berndtsson, who also provided access to relevant data from the technical specifications.

References

[1] Peschel J *Achterbahnbremsen - Von der Reib- zur Wirbelstrombremse* Coasters and More http://www.coastersandmore.de/rides/brake/brake.shtml
[2] Marden D, *Roller Coaster Data Base* http://www.rcdb.com
[3] Peschel J *Kanonen - Great Firepower at Liseberg* Coasters and More http://www.coastersandmore.de/rides/kanonen/kanonen.shtml
[4] Ho C Y *et al* 1983 *Electric resistivity of ten selected binary alloy systems* J. Phys. Chem. Ref. Data **12** 183-322, www.nist.gov/data/PDFfiles/jpcrd221.pdf
[5] A movie sequence of the heating and cooling of the brakes is available at stacks.iop.org/PhysED/47/000000/mmedia.
[6] Wiederick H D, Gauthier N, Campbell D A and Rochon P 1987, *Magnetic braking: Simple theory and experiment* American Journal of Physics, 06/1987, **55** p. 500
[7] Pendrill A-M 2008, *Acceleration in 1, 2, and 3 dimensions in launched roller coasters*, Physics Education **43** 483-491

[8] Heintz V, Mårtensson Pendrill A-M, Schmitt A and Wendt, K (2009) *Achterbahn fahren im Physikunterricht* Physik in unserer Zeit, 40:2 90-95

[9] Pendrill A-M and Rödjegård H 2005, *A roller coaster viewed through motion tracker data* Physics Education **40** 522-526

Appendix A. Dimensionless equations of motion and analytical solution

Equation 1 describing the braking in a magnetic brake is analogous to the equation

$$y'' = -2y'y \tag{A.1}$$

Using Mathematica, we were able to solve this non-linear differential equation, giving

$$y(x) = tanh(x) \tag{A.2}$$

To make use of this analytical solution, we rewrite equation (1) in terms of dimensionless variables, e.g. as

$$a/\sqrt{kv_0^3} = -2(v/v_0)(s\sqrt{k/v_0}) \tag{A.3}$$

The analytical solution to this equation can be written as

$$s(t) = \sqrt{2v_0/k}\tanh(\sqrt{kv_0/2}t) \tag{A.4}$$

Since the maximum values of the tanh function is 1, we find that the maximum distance travelled is

$$D = \sqrt{2v_0/k} \tag{A.5}$$

The velocity is found by taking the time derivative of Eq. (A.4), which gives

$$v(t) = \frac{d}{dt}s(t) = v_0\ \mathrm{sech}^2(\sqrt{kv_0/2}t) \tag{A.6}$$

where $sech(0) = 1$ gives the numerical value for the initial velocity, $v(0) = v_0$. (The factor 2 in the analytical equation (A.1) is needed to get this simple relation.)

For completeness, we give also the expression for the acceleration of the train:

$$a(t) = -\sqrt{2kv_0}\tanh(\sqrt{kv_0/2}t)\mathrm{sech}^2(\sqrt{kv_0/2}t)$$

Using transformations to dimensionless variables, the different graphs in figure 3 can be reduced to a single graph with the dimensionless variables on the axes. Figure 4 shows how velocity and acceleration depends on the distance travelled, but expressed in terms of the dimensionless variables $y = s\sqrt{2k/v_0}$, $y' = v/v_0$ and $y'' = a\sqrt{8/kv_0^3}$. The dimensionless variable involving the time is given by $t\sqrt{kv_0/2}$.

Appendix B. Temperature distribution over the brakes

In this Appendix we model the distribution of the temperature change in the brakes, assuming that the energy is distributed evenly over the height, h, of the track, as well as over the thickness, b. The reduction in kinetic energy as the train moves a distance ds can be written as $dE_k = mv\ dv = ma\ ds$. Neglecting first the complication that the train is no longer in contact with the first brake fin at the end of the stopping distance, we find that the energy deposited per length unit of the brakes is $-dE_k/s = ma\ ds/s = -m(kvs)\ ds/s = -mkv\ ds$ for the active part of the brake. For the temperature increase, we need to know the energy deposited per mass of the brake fin as the train moves a distance , i.e. $dT = dQ/(CM) = dQ/(2C\rho hbs)$, where the factor 2 is needed to account for the two fins in the brakes.

$$\Delta T(x) = \frac{mk}{2C\ \rho\ h\ b} \int_x^D v\ ds. \tag{B.1}$$

From the analytical solution in section 3, we can use figure 4 to estimate the temperature increase of the first brake fin. The integral over the whole area, using dimensionless variables becomes $\int_0^1 y'\ dy = \int_0^\infty (y')^2\ dt = 2/3$. Alternatively, the derivative of $\tanh(x)$ can be evaluated explicitly, giving $y' = (1 - y^2)$. The integral can then be rewritten as

$$\int_0^1 y'\ dy = \int_0^1 (1 - y^2)\ dy = 2/3.$$

Insertion of the parameters from the expressions for s and v in Eqs (A.4, A.6), gives the temperature increase at the beginning of the brake:

$$\Delta T(0) = \frac{mk}{2\ C\ \rho\ h\ b}\ v_0\sqrt{\frac{2v_0}{k}}\ \frac{2}{3} = \frac{m}{3\ C\ \rho hb}\ \sqrt{k2v_0^3}.$$

The expression above would hold for a horizontal track, with train and brakes at least as long as the stopping distance, $D = \sqrt{2v_0/k}$, and assuming that all the kinetic energy of the train is absorbed by the brake fins. We note that $dT(0)$ is proportional to $v_0^{3/2}$ rather than to v^2, as the kinetic energy. The remaning factor $v_0^{1/2}$ comes from the longer stopping distance (A.5) for an increased initial speed.

To compensate for the final part of the brake, when the train of length L_t is no longer close to the part of the braking fin at position x, the contribution from the tail can be subtracted, giving a slightly reduced rise in temperature, $\Delta T_c(x) = \Delta T(x) - \Delta T(L_t + x)$.

Inserting numerical values for Kanonen, we find in this way $\Delta T(0) = 12.8K$. Figure 7 shows the expected distribution of temperature increase over the brake fins, with and without this tail correction. The upper curve in figure 7 starts slightly higher than the analytical value for $dT(0)$, reflecting the added energy due to the 4.3^o slope of track.

Appendix C. Authors

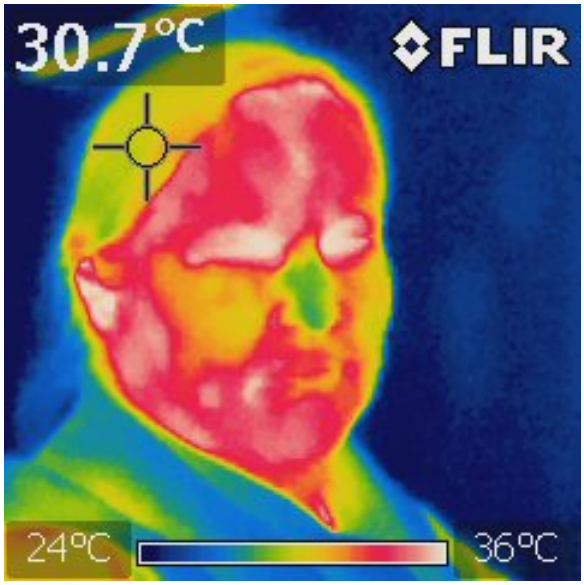

Figure C1. Ann-Marie Pendrill is professor of physics at University of Gothenburg with a research background in computational atomic physics. Since 2009, she is also the director of the Swedish National Resource Centre for Physics Education, hosted by Lund university. She has arranged amusement park science days, and used examples from playgrounds and amusement rides in the education of physics, teaching and engineering students.

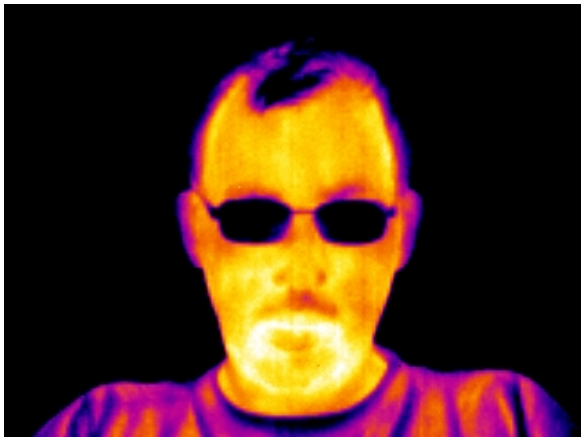

Figure C2. Magnus Karlsteen is associate professor of applied physics at Chalmers University of Technology.

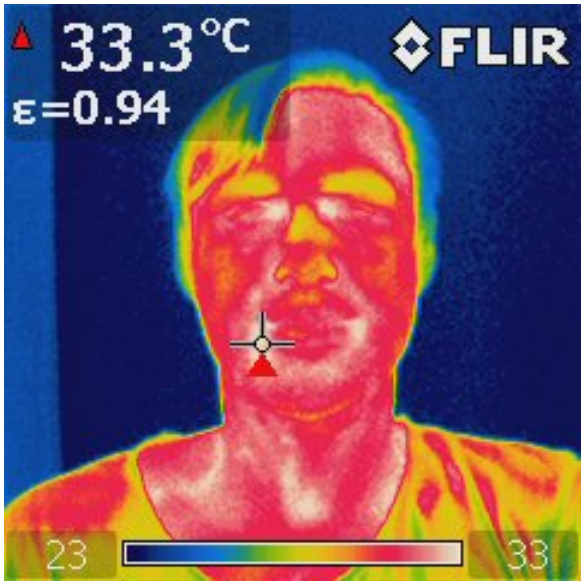

Figure C3. Henrik Rödjegård has a Ph.D. in Solid State Electronics. In his research he has focused on development of micro-sensor components and electronic systems for these. The electronics research has includes construction and verification of several analogue integrated circuits for readout of various sensor signals. Since 2006 he has been working with research related to development of gas sensors based on infra-red detection.